Reports of the Department of Mathematical Information Technology
Series B. Scientific Computing
No. B 1/2016

A Review of the Analytical and Numerical Modeling of Composites

Anna-Leena Erkkilä Tero Tuovinen
Matti Kurki

University of Jyväskylä
Department of Mathematical Information Technology
P.O. Box 35 (Agora)
FI–40014 University of Jyväskylä
FINLAND
fax +358 14 260 2209
http://www.mit.jyu.fi/

ISBN 978-951-39-6528-0 (nid.)
ISBN 978-951-39-6935-6 (PDF)
ISSN 1456-436X

A Review of the Analytical and Numerical Modeling of Composites *

Anna-Leena Erkkilä[†] Tero Tuovinen[‡] Matti Kurki[§]

Abstract

This review article is dedicated to the materials that are made from two or more constituent materials with different physical and/or chemical properties. The focus is on the materials, where the individual components remain separate and distinct within the final structure. The new combined material usually have some additional characteristic properties compared to the individual components, or, in other case, some critical properties of combined material may follow almost equally one of the components. Typically, preferred properties of the new material can be such as strength, porosity, conductivity or cheapness. The ultimate goal of this study is to find methods and tools for achieve adequate strength even when the low quality component is added to primary material or when two or more 'waste' matters are combined with each other in novel industrial processes. Contribution of this article is to review modeling possibilities of different composite materials and bring out new ideas to model composites including low quality or waste materials.

1 Introduction

The science and technology of composite materials receives much attention arising from composite's ability to provide novel and specific properties that exactly meets the requirements of various industrial applications ranging from aerospace to bio-medical areas. Nature is full of examples of composite materials and the idea of man-made composite materials is not a novel. Typical engineered composite materials can include cements, concrete, asphalt concrete, fiber-reinforced polymers, fiber-reinforced thermoplastics, metal composites, ceramic-metal composites, glass-reinforced plastic, carbon-fiber-reinforced polymer, hemicellulose based composites, etc. In this review we restrict our study to manufactured composites, which are formed by combining two or more physically and/or chemically distinct, suitably distributed and arranged phases with an interface separating them. There is

*Report for the project Recycling and Utilization of Waste Matter and Sludge Components
[†]Department of Mathematical Information Technology, University of Jyväskylä, Finland
[‡]Department of Mathematical Information Technology, University of Jyväskylä, Finland
[§]JAMK University of Applied Sciences, Jyväskylä, Finland

large variety of subjects, such as macro, micro and nano structure of composite; the mechanics – interface, fatigue, environmental interactions – and process modeling, which are under discussion in scientific and engineering community. In this article we are looking the field from mathematical modeling point of view, and therefore we have divided the composites into five categories based on their structural behavior or production technology. The categorization is not meant to constrict the generation of ideas, but to provide fluent basis for different point of views on the topic. The categories and products belonging to them are overlapping and some materials may have properties of two or even more groups.

The materials have been categorized as follows:

1. Reinforced materials.
2. Matrix with weakening components or pores.
3. Two material matrices combined together.
4. Heterogeneous materials.
5. Laminates and sandwich-structured composites.

Detailed description with examples of each category is defined in Table 1. Most composites are usually considered to belong to categories 1 or 5. In categories 1 and 2, the matrix is considered the primary phase, and discontinuous dispersed phase secondary. The primary phase (matrix) is generally responsible for providing the bulk form of the material as a whole.

There are several aspects when considering the mathematical modeling of composite materials. The behavior of composite materials is determined by the relevant material properties of the constituents and by their geometrical arrangement. The constituents may also have different shrinkage and thermal expansions or the moisture and humidity may affect them differently. This may cause internal stresses and their energy may dissipate during the failure process through micro-cracks. The primary and secondary material are usually bonded together through interface, which behavior can be crucial for understanding and for fully determining the mechanical behavior of composite.

An usual aim of mechanical studies of heterogeneous materials attends to estimate their overall, effective or apparent, behavior (e.g., stiffness, fracture or strength properties). The homogenization techniques are commonly used in continuum micromechanics of the materials. The Representative Volume Element (RVE) with effective parameters (e.g., effective moduli, effective stress or effective strain) and asymptotic methods are typical concepts. In these models, the effective properties of a unit cell of the material at the lower scales are determined and used in the higher scales (see, e.g., Zaoui (2002)). The other commonly used method family is called Micro Finite Element Analysis techniques (μFEA). In these methods the number of elements is increased and the size of elements is decreased. The drawback is that these models require substantial computational resources and time. Recently, the multiscale element models have been in the focus of the latest achievements. They may

Table 1: Five categories of different kind of composites based on mathematical modeling point of view.

Category	Description
Category 1	Composites having a primary material forming a basic matrix, where some other material(s) is (are) used to reinforcement or otherwise to improve the properties. The primary phase encloses or surrounds the secondary phase, and shares or transfers imposed mechanical load to and from the reinforcing phase. The reinforcing phase material may be in the form of discontinuous flakes, particles, fibers, whiskers, or nanoparticles. Common matrices include mud (wattle-and-daub), cement (concrete), polymers (fiber reinforced plastics), metals, ceramics, bitumen (asphalt concrete) and even some unusual matrices, such as ice (pykrete).
Category 2	The materials in category 2 are very much alike as in category 1, but the material matrix includes dispersed secondary particles (fillers), which instead of working as reinforcement decrease the mechanical properties of primary material. Usually these filler materials are added, because they are cheaper than the main material, or they are impurities that can not be extracted from raw material. The typical printing paper is an example of a composite of this category having cellulose fiber matrix and filler particles, such as $CaCO_3$. The filler decreases price, improve opacity and control gloss, but when used at high amounts, it decrease the tensile and thickness directional strength of paper. Broadly speaking, the porosity of matrix can be seen as one of the examples of this category.
Category 3	Materials in category 3 are again very much alike as in category 1, but there is two matrix combined and mixed together, i.e. the reinforcing or secondary phase material has a continuous nature. For example, there might be wood fiber network containing long fibers or woven mats of fiber and then some other material, such as ceramic matrix. Wire mesh glass is a representative example.
	Continued on next page

Table 1: (continued)

Category	Description
Category 4	Composite as a heterogeneous structure, where different materials are chemically bonded with each other. These structures may be processed by adhesive pressing and particle bonding. Particles may be self-binding, or heat (hot-pressing), binding adjacent, adhesives or additives may be used. Examples: particleboard and some wood plastic composites formed by extruding.
Category 5	Laminates consist of multiple layers. Composite laminates consist of fibers in a polymeric metallic or ceramic matrix material. Layers of different materials may be used, resulting in a hybrid laminate. The individual layers generally are orthotropic or transversely isotropic. Sandwich-structured composites are composite material that is fabricated by attaching two thin surface layers to a lightweight thick core. They are widely used in aerospace structure, infrastructure, etc. The light-weight core materials are, for example, foam, truss and honeycomb core. The corrugated fiberboard boxes are examples of laminated structures and sandwich structured composites. Many paper grades are coated and can also be considered as laminates.

include ability to select adaptively the intermediate level that is most suitable for a given problem (see, e.g., Liu et al. (2006)). Analytical approaches and regression models based on empirical data are also common. Some special treatments for crack propagation and interface region are also introduced.

2 State of art of the categories

In this section, description of common composite modeling schemes and several examples of modeling of the categorized composite structures are presented. Empirical, semi-empirical, analytical and numerical models are all considered. Reviewed applications include industrial products such as rubber-carbon black, concrete, steel and steel fiber reinforced concrete and polymer matrix and different flake boards. Also analytical micromechanial models for fiber composite and porous structures, and laminate models are briefly reviewed.

2.1 Category 1: Reinforced materials

The materials in category 1 contain the primary material forming a basic matrix while some secondary material(s) is(are) used to reinforcement or otherwise to improve properties of composite. Firstly, a theory of filler reinforcement for the stiffening of elastomers is presented, and secondly, analytical micromechanical models for fiber composites are briefly reviewed in this section. Softening modeling of concrete have been under extensive development for decades and was chosen as an application to represent a quasi-brittle material. Brief glance on few examples of fiber reinforced concretes and fiber reinforced polymer matrix as a high ductility and stiffness materials are also provided in this section.

2.1.1 Theory of filler reinforcement

Rigid fillers can usually be used to increase the stiffness of an elastomeric material. Guth (1939) modified the Einstein's viscosity law (Einstein (1906, 1911)) to predict the small strain modulus of rubber-carbon black system considering carbon black spheres as suspended in a continuous rubber matrix. In the model an additional term to account for the interaction of fillers at larger filler volume fractions was included. In the article Guth (1945), the model was generalized for ellipsoidal filler particles and was extended to the various properties of the matrix and the fillers. Young's modulus and stress-strain curve were derived as a functions of the volume concentration c and compared to experimental studies.

2.1.2 Stiffness predictions for fiber composites, analytical micromechanical models

The simplest treatment of the elastic behavior of aligned long-fiber composites is simply based on a weighted mean between the moduli of the two components, depending only on the volume fraction of fibers. This Rule of Mixtures (ROM) provides two theoretical models: Voigt model (Voigt (1889)) for upper-bound axial loading and Reuss model (Reuss (1929)) for lower-bound transverse loading. Also Poisson's ratio and shear modulus can be derived by following the rules of mixture, and Kim et al. (2001) used the ROM to predict the plastic flow curves for various volume fractions of the soft and hard particles. Accurate experimental validation of the longitudinal model has been demonstrate for a number of composites with continuous fibers, while the transverse model is generally known as being inadequate for predicting the transverse modulus. Hashin & Shtrikman (1963) construct the tighter bounds, in which single variational principle gives both the upper and lower bounds by making appropriate choices of the reference material. Widely used semi-empirical Halpin-Tsai equations (Halpin & Kardos (1976)) were developed to correct the transverse Young's modulus and shear modulus, and also to obtain generalized model for predicting properties of short-fiber composites. Halpin's and Tsai's derivation for the analytical form of equations was based on Hermans solution (Hermans (1967)) of the self consistent micromechanical model developed by Hill (1964), while fiber geometry have accounted through the use of empirical factors.

For short-fiber composites, the fundamental result used in several different models is Eshelby's solution for ellipsoidal fibers in dilute concentrations fractions (Eshelby (1957)). The key result was to show that within an ellipsoidal inclusion the strain is uniform, and is related to transformation strain by so called Eshelby's tension, which depends only the inclusion aspect ratio and the matrix elastic constants. A detailed derivation and applications are presented in Murakami (1988).

For non-dilute concentrations, for example, Mori-Tanaka (Mori & Tanaka (1973), Benveniste (1987)) and self-consistent methods (Hill (1965), Budiansky (1965)) are presented. In the Mori-Tanaka method the Eshelby approach was combined with the effective field concept by defining strain concentration tensor, which relates the strain in inclusion to a far-field strain equal to the appropriate average strain in the matrix. Tandon & Weng (1984) developed equations for the complete set of elastic constants of the a short-fiber composite based on Mori-Tanaka approach. For the computation of the transformation strain in the self-consistent methods the single particle is embedded in the effective medium of composite, which properties are not known a priori. The original work focused on spherical particles and continuous aligned fibers, but approaches for short fiber composite is developed, see, e.g., Chou et al. (1980).

Shear lag model developed for paper and fibrous materials (Cox (1952)) analyzes the transfer of tensile stress between the fiber and the matrix by means of interfacial shear stress. In shear lag models the mechanical properties of composite can be expressed as a function of the volume fraction and aspect ratio of fibers (Fukuda & Chou (1982)).

2.1.3 Numerical models for crack propagation in concrete

As an application in this category the vastly used, studied and modeled concrete is presented. The concrete is a quasi-brittle composite material made of aggregates (coarse gravel, crushed rocks and sand) and cement paste. The mechanical behavior of concrete is complex and nonlinear in both tension and compression. The dominant mechanism of concrete material response to loading is the initiation and propagation of cracks. The stiffness degradation is mainly due the material damage: initially invisible micro-cracks caused by shrinkage, thermal expansion and other phenomena will progress to visible cracks under external loads. Failure accumulates through micro-cracks, which are formed due to the cohesion loss between the mortar and the aggregate, at interface between the aggregate and the mortar due the frictional slip, or crushing of the mortar (Nguyen (2005)).

In uniaxial loading, the experimentally observed deformation process is different in tension and compression. In a compressive test the cracks are parallel to the direction of the compressive stress, while in a tensile test the direction of crack propagation is transverse to the stress direction. Under severe loading (beyond the peak stress), concrete exhibits a strain-softening response, in both tension and compression (see Figures 1 and 2) (Gopalaratnam & Shah (1985)). The experimental observations obtained from the uniaxial tensile and compressive behavior of the concrete can also be applied to multi-axial stress states (Chen & Han (2007)). Two separate kinds of envelopes are used to characterize the concrete behavior in stress stages: the elastic region is defined by the elastic-limit surface, and the maximum-strength envelope of the concrete is characterized by the failure surface, see Figure 3. The softening is a combined material/structural property and the stiffness degradation in concrete is mainly caused by the material damage especially in the post-peak situation (Chen & Han (2007)).

The structure and properties of concrete such as the shape, size and surface structure of aggregates, the water-cement ratio, the used type of cement, and other factors have influence on behavior of the product. Nevertheless, a concrete is often simulated using macroscopic models, where a concrete is treated as a continuum, and behavior caused by the heterogeneous material structure are included in the constitutive law (see, e.g., Nguyen (2005), Lemaitre (1992)). As the behavior of quasi-brittle material is considered, the major focus has been on the fracture studies i.e. situations where material is subjected to moderate to severe loading and crack develops and propagates. Main approaches of the continuum modeling for crack propagation can be categorized as the discrete crack approach, the smeared crack approach, non-local fracturing theory, damage mechanics and lattice models.

In the discrete crack approach the aim is in simulation the initiation and propagation of dominant cracks and thus is preferred approach when the structure contains one or a finite number of cracks (Ngo & Scordelis (1967)). It was recognized in early studies that the stress and strain fields that are developed at the tip of the crack are singular and stress criteria were not reliable. The cohesive crack model, developed by Hillerborg et al. (1976) for crack propagation of concrete introduces fracture process zone (FPZ) locating ahead of the macro-cracks. Significant amount of energy is

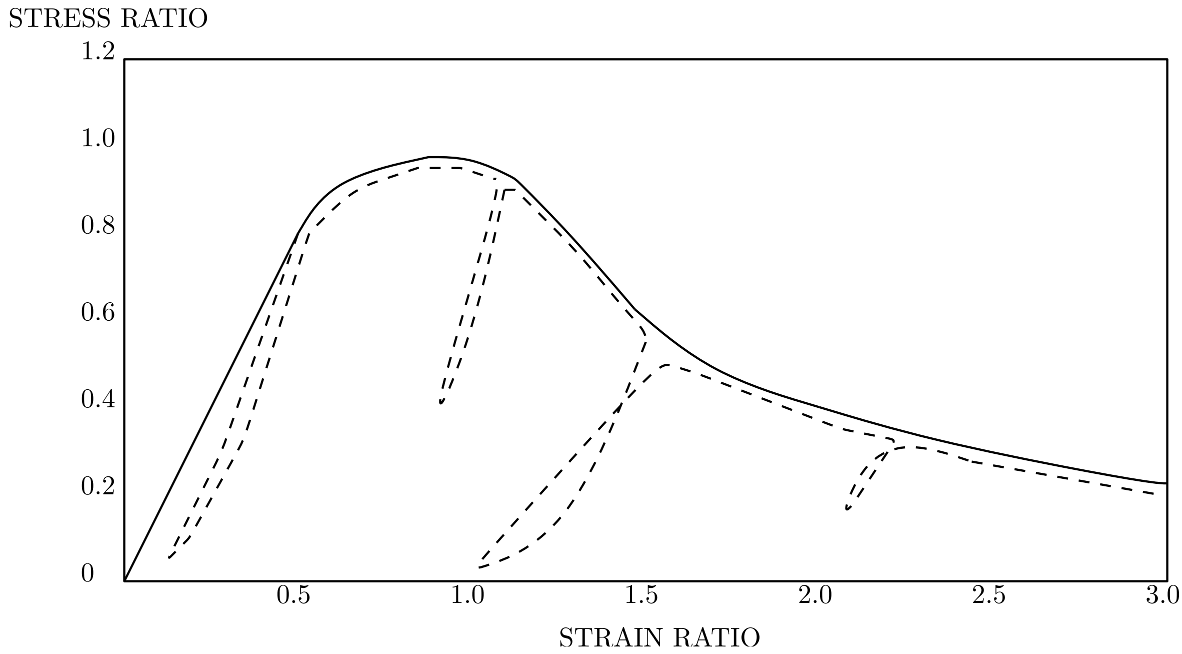

Figure 1: Stress-strain behavior of concrete subjected to monotonic and cyclic compression. (Schematic figure after Bahn & Hsu (1998))

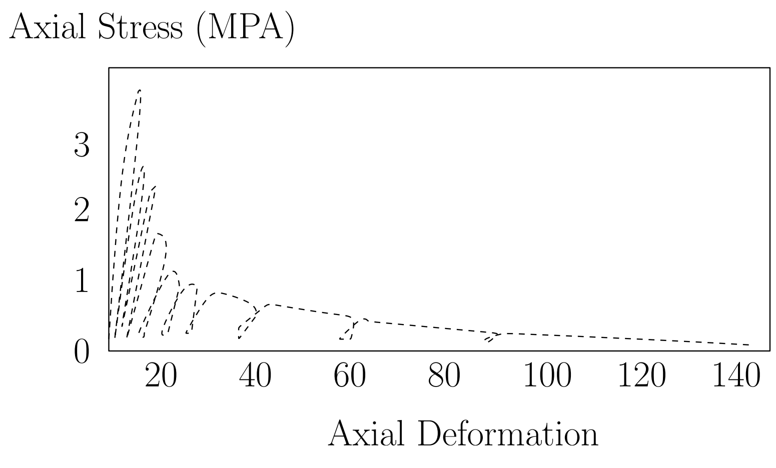

Figure 2: Stress-deformation curve of concrete under uniaxial cyclic tensile loading. (Schematic figure after Reinhardt et al. (1986))

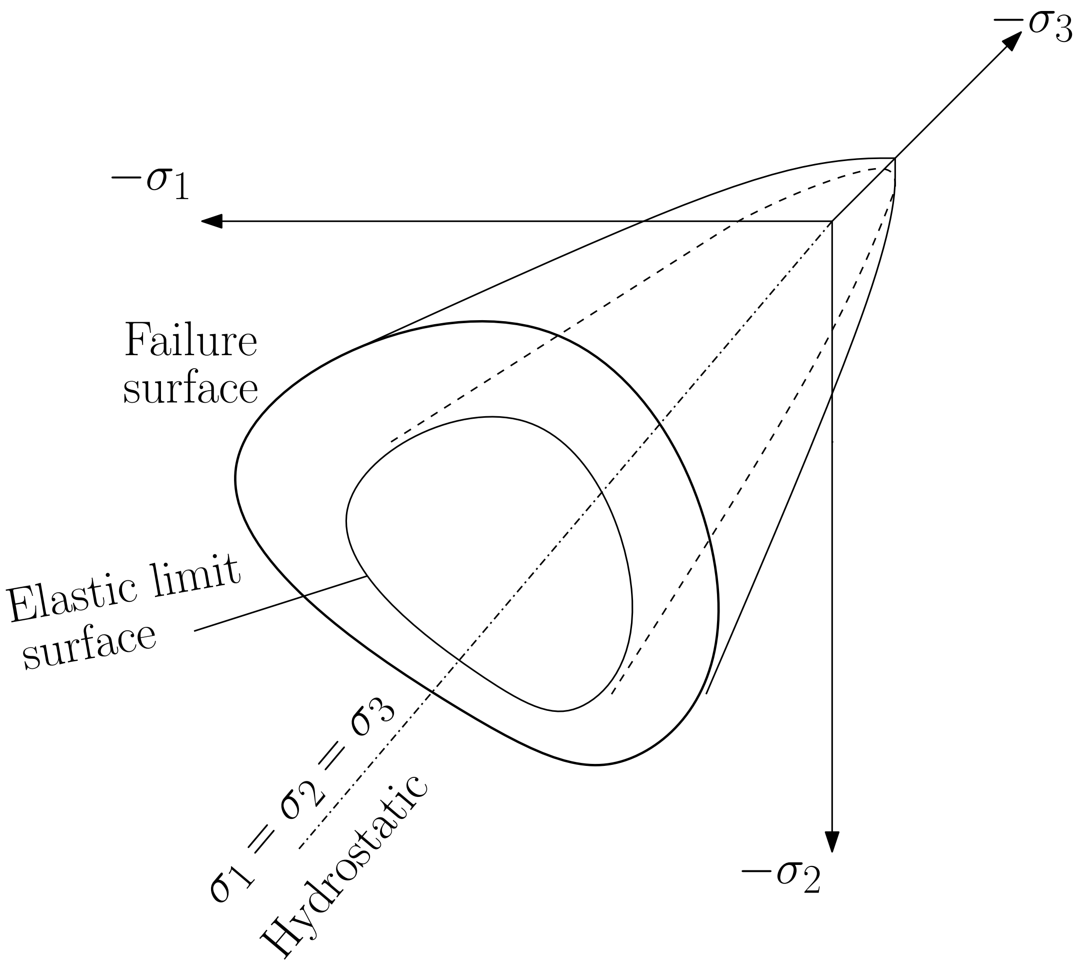

Figure 3: Failure and elastic limit surfaces in principal stress space. (Schematic figure after Chen & Han (2007))

stored in that large FPZ region, containing micro-cracks in which case a crack can have stable growth before peak load. Cohesive stress as a function of crack opening reaches tensile strength at the tip of the crack and reduces to zero when there is the critical opening of the crack. The area under the softening stress-separation curve is equal to the energy release rate of the structure. The propagation of discrete cracks through elements requires the refinement and re-meshing of the finite element mesh. Meshless methods, such as element-free Galerkin methods, have also been applied to avoid difficulties for constant redefinition of the mesh topology (see, e.g., Belytschko et al. (1994), Dong et al. (2010)). Recently, so-called extended finite element method (X-FEM) (Sukumar et al. (2000)) and strong discontinuity approach (Oliver & Huespe (2004)) have been introduced to overcome disadvantages of the discrete crack approach and avoiding need of remeshing. One of the challenges associated with discrete crack models are that they require material properties that are difficult to measure.

In the smeared crack approach the cracked material is assumed to remain a continuum as an infinite number of cracks are theoretically distributed (smeared) over the element (Rashid (1968)). The propagation of cracks is modeled as the reduction of the strength and stiffness. The result is non-linear constitutive models with elastic degradation and/or softening plasticity (see, e.g., Bažant & Planas (1998), Carol & Bažant (1997), Weihe et al. (1998), Ohmenhauser et al. (1999), de Borst (2002)). The smeared crack approach was first introduced by Rashid (1968). Bažant & Oh (1983a) proposed crack band model based on work of Hillerborg et al. (1976) to solve unphysical mesh size sensitivity which is consequence when the strain softening is considered as a characteristic of the material. In the crack band model the dissipated energy in strain softening is related to the fracture energy of the material.

The non-local models are based on the continuum mechanics, where the evolution of stress and changes at the micro-structural level due the loading are based on such a theories as plasticity and damage mechanics. Dougill introduced the progressive fracturing theory which involved the stiffness lose of the material due to progressive fracturing during the deformation process (Dougill (1976)). In this approach the material return to a state of zero strain at zero stress by linear elastic unloading. This is based on theoretical assumption that the microcracks are in principle able to close and no residual strain will remain in the material after unloading to zero stress. However, in real material some residual strains after unloading are prevailing, since during crack formation some particles loosen from the crack edge prevent the complete closure of the microcracks. Based on the work of Dougill the elasto-plastic-fracturing theory for concrete was carried out by Bažant & Kim (1979).

Continuum damage mechanics (CDM) was first proposed for creep rupture of metals by Kachanov (1958, 1999) and it have become one of the classical tools of the structural mechanics and concrete modeling, see, e.g., Lemaitre & Chaboche (1990), Faria et al. (1998), Peerlings (1999), Jirásek & Patzák (2001), Jirásek et al. (2004), Luccioni et al. (1996), Comi & Perego (2001), Comi (2001), Salari et al. (2004), Nguyen (2005), Genet et al. (2014). Damage theories provide an effective way to characterize the microscopic deterioration of material by the macroscopic level variables.

The coupling between damage evolution and strain is usually formulated to obey the irreversible thermodynamic laws, though in principle damage theory can be developed by setting a stress-strain law related to damage and a yield/damage limit function (see, e.g., Lee & Fenves (1998), Addessi et al. (2002)). From the thermo-mechanical point of view, the input energy is dissipated during the failure evolution through micro-cracks (Nguyen (2005)). In CDM the definition of damage indicator, such as presented by Lemaitre (1992), are used to characterize the form of the stiffness reduction covering the thermodynamic, micro-mechanical and geometrical aspects of the macroscopic representation of the material deterioration. The simple scalar damage variable is obtained by measuring the area of the intersection of all defects in selected plane and by dividing that area S_D with total area of that plane S, i.e. damage variable $D_n = S_D/S$, see, e.g., Lemaitre (1984). A scalar damage variable was first used to describe isotropic damaging, but because the damage of concrete caused by microcracks is usually oriented leading to anisotropic damage, the damage tensors of higher order are introduced, see, e.g., Kachanov (1980), Krajcinovic (1985), Murakami (1988), Simo & Ju (1987). The internal state variables can be developed within two alternative frameworks: strain-based or stress-based formulation (Simo & Ju (1987)). In Nguyen (2005), the author presented a formulation of elasto-plastic damage constitutive model based on the use of thermodynamic potentials proposed by Houlsby & Puzrin (2000). The strain softening and stiffness degradation was modeled by damage mechanics, while the residual strains and some other macroscopic features are related to and captured by plasticity theory.

The components of the damage tensors of second, fourth or even eight order (see, e.g., Lemaitre & Chaboche (1990)) are very difficult to identify. The alternative approach to the tensorial damage formulation, the so-called microplane model have been proposed by Bazant and Oh (Bažant & Oh (1983b), Bažant & Gambarova (1984)) based on work of Taylor (1938) on plasticity of crystalline metals. In a microplane model the material behavior is modeled in planes of all possible orientation through uniaxial stress-strain laws and in terms of stress and strain vectors (see Figure 4). The microplane strain and stress vectors are related to the continuum tensors by a kinematic constraint and variational principle. The microplane model for concrete has passed many stages of developments labeled M0,M1,...,M7, see, e.g., Bažant & Prat (1988), Bažant et al. (2000), Bažant & Caner (2005), Caner & Bažant (2012). The improvement between stages have been concentrated in tensile cracking and postpeak tensile softening, simultaneous modeling of tensile and compressive failures, formulation of boundary surfaces and frictional yield limits, creep and arbitrary large finite strain. In model M2 a volumetric-deviatoric split of the normal strains and stresses on the microplanes was introduced to help to control triaxial phenomenon of compression failure. In stage M7 the volumetric-deviatoric split for the elastic part and for the tensile boundary were abandoned while it was retained for the deviatoric stress-strain and compressive normal boundaries, which sum is then compared with the total normal stress.

In lattice models, the continuum is discretized as a lattices or mesh of truss or beam elements that transfer forces and which may have different properties, de-

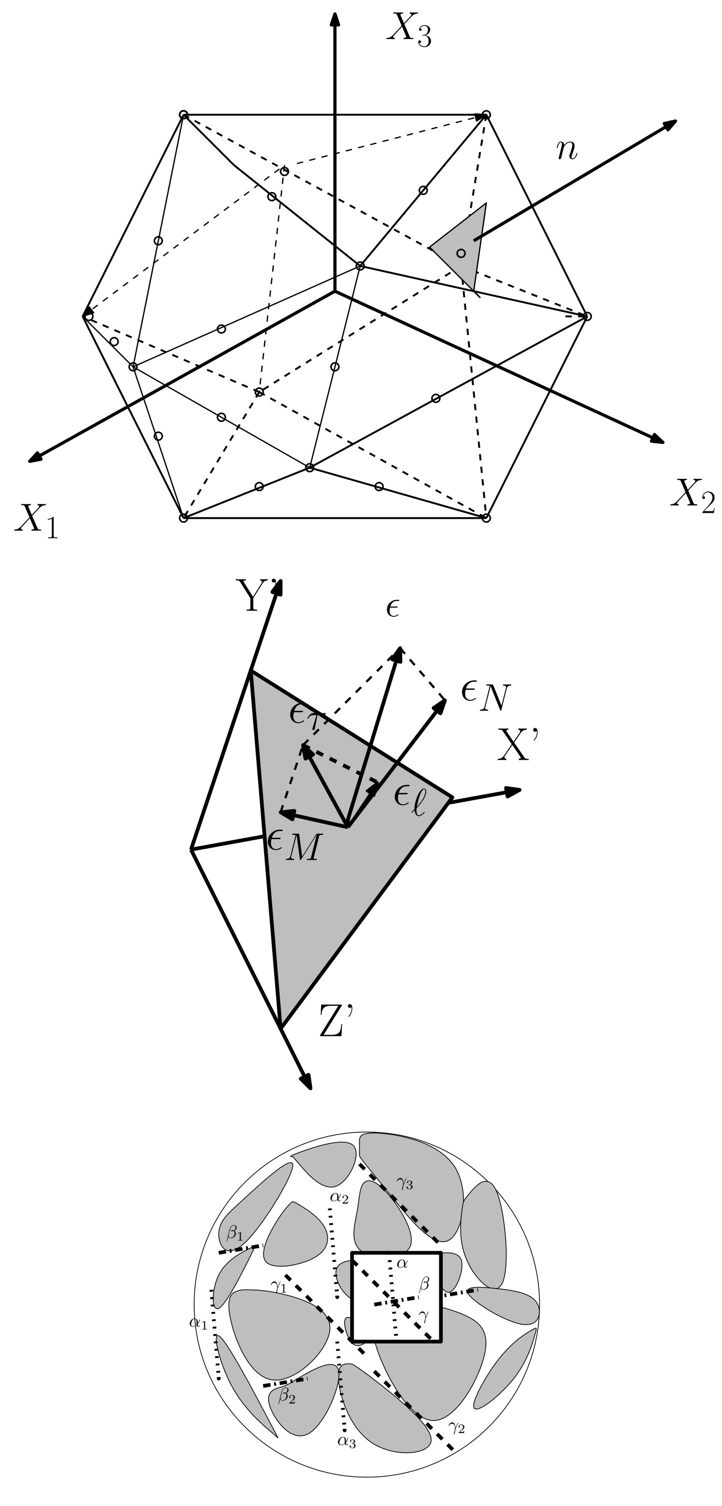

Figure 4: Top: Example of 21-point optimal Gaussian integration formula. The circled points represent the directions of the microplane normals. Middle: Consequential microplane model after separate homogenization of slips and openings on weak planes $\alpha_1,\ \alpha_2,\ldots$ of various orientations $\alpha,\ \beta,\ \gamma,$... within the representative volume. Bottom: Microplane strain components. (Reproduced from Caner et al. (2013))

pending on weather the element represents a cement paste matrix, aggregate or interfacial zone (Schlangen & Van Mier (1992b), Lilliu & van Mier (2003)). Fracture is simulated by a linear elastic analysis of the lattice under loading and eliminating (or partially eliminating) an element that exceeds a criteria threshold of quantities such as strength or energy from the mesh. The weak interface found between the aggregates and the cement paste matrix can be treated in simulation by adjusting the tensile strength and the modulus of beams or truss that located in this region, as well as permitting for differences between aggregates and cement paste matrix (Schlangen & Van Mier (1992a), Cusatis et al. (2003)). The softening can be introduced at element level or based on elastic purely brittle fracture criterion. The results obtained can depend strongly on the chosen element or mesh type and the fracture criterion used. The randomness of lattice is also important to avoid bias in crack propagation direction. Lattice models assume usually a linear-elastic material constitutive relation and are two-dimensional although some three-dimensional versions have been introduced for concrete modeling (Lilliu & van Mier (2003)). Cusatis et al. (2011) introduced lattice discrete particle model (LDPM), which is synthesis of confinement shear lattice model and discrete particle models presented in Cusatis et al. (2003) and Pelessone (2005), respectively. LDPM simulates concrete by system of interacting aggregate particles connected by a lattice system that is obtained through a three dimensional Delaunay tetrahedralization of the aggregate centers. The constitutive behavior is softening for tension and shear-tension and plastic hardening for compression and shear-compression.

2.1.4 Steel fiber reinforced concrete

The fibers can be used to strengthen the cementitious matrix of concrete, since they restrict and delay the progression of microcracks into wide continuous cracks. Especially, steel fibers enhances ductility and energy absorption capability. In the steel fiber reinforced cementitious composite, the mechanical behavior depends on the interfacial bonding, fiber pull-out, fiber and matrix properties, the fiber orientation and their dispersion in the matrix, flaw size and distribution, etc. (Pereira (2006)).

Ramadoss & Nagamani (2012) present the empirical linear regression models to evaluate the strength and toughness of High Performance Steel Fiber Reinforced Concrete (HPSFRC). The estimated parameters were compressive strength, modulus of rupture, splitting tensile strength and toughness ratio. The eight variables defining the mixture proportions of 144 composite specimens (water–cementitious materials ratio, steel fiber volume fraction, superplasticizer dosage, and weight of cement, fine aggregate, coarse aggregate, water and silica fume) were used in regression analysis.

Leite et al. (2004, 2007) applied a mesoscale lattice model for fracture process studies of concrete and fiber reinforced concrete. The effort was made to create a structural distribution of aggregates and cement paste matrix in a realistic way. The stochastic-heuristic algorithm was introduced for this purpose. The generated three-dimensional structure specimens were discretized into lattices of linear elements for

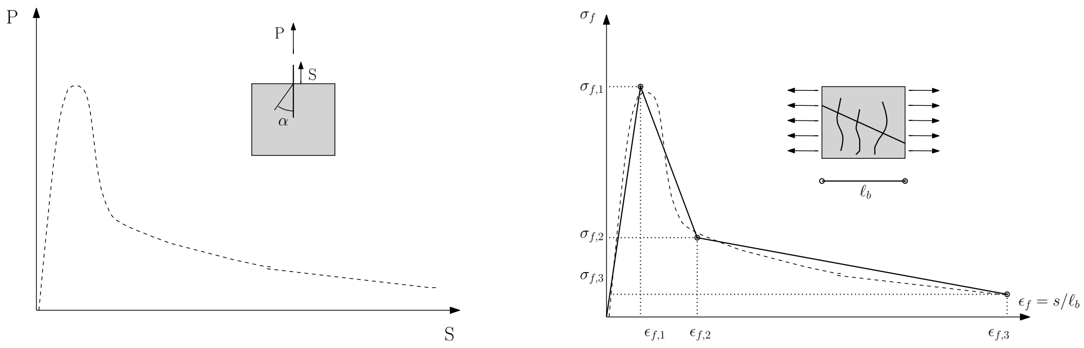

Figure 5: Procedure to obtain pullout parameters from the experimental force-slip relationship in Cunha et al. (2011). (Reproduced from Cunha et al. (2011))

both two-dimensional and three-dimensional analysis. After the aggregate-matrix structure were generated, the fibers were allocated directly into the mesh for fiber reinforcement modeling. Additional elements connecting distant mesh nodes in the cement matrix was introduced. The different softening laws in tension and compression was implemented into the constitutive laws of the elements corresponding either aggregate, matrix or interface. The softening of elements representing fibers was described by the bond-slip relation.

In model presented in the article Cunha et al. (2011) for Steel Fibre Reinforced Self-Compacting Concrete (SFRSCC), a two phase material is assumed. Heterogeneous concrete medium is treated as one homogeneous phase and another phase is composed of steel fibers. The fracture process of the concrete phase is modeled by a three-dimensional smeared crack model and discretized by solid finite elements. The random distribution of short cables imitating steel fibers is simulated using Monte Carlo method and the geometry, position and orientation of the fibers are subsequently inserted in a finite element mesh. The fibers are embedded in the concrete matrix as a three-dimensional truss elements to model the stress transfer between crack planes due to the fibers bridging a progressive crack. The bond–slip behavior of the steel fibers was derived from the experimental pullout stress–slip relationship (Figure 5).

The microplane models M5 and M7 for concrete, presented in previous chapter, have been generalized for simulation of fiber reinforced concrete in references Beghini et al. (2007) and Caner et al. (2013). For fiber reinforced concrete model M5f the softening law of stress–strain boundaries of concrete model M5 is modified to enhance ductility. The coupling of kinematically and constrained microplane systems allows simulating the evolution of microcracks of many orientations into wide cracks of one distinct orientation. More realistic determination of the fiber pullout and breakage was brought to microplane model M7f to model fiber reinforced concrete including gradual activation of fibers bridging an opened crack as is presented in Figure 6 (Caner et al. (2013)).

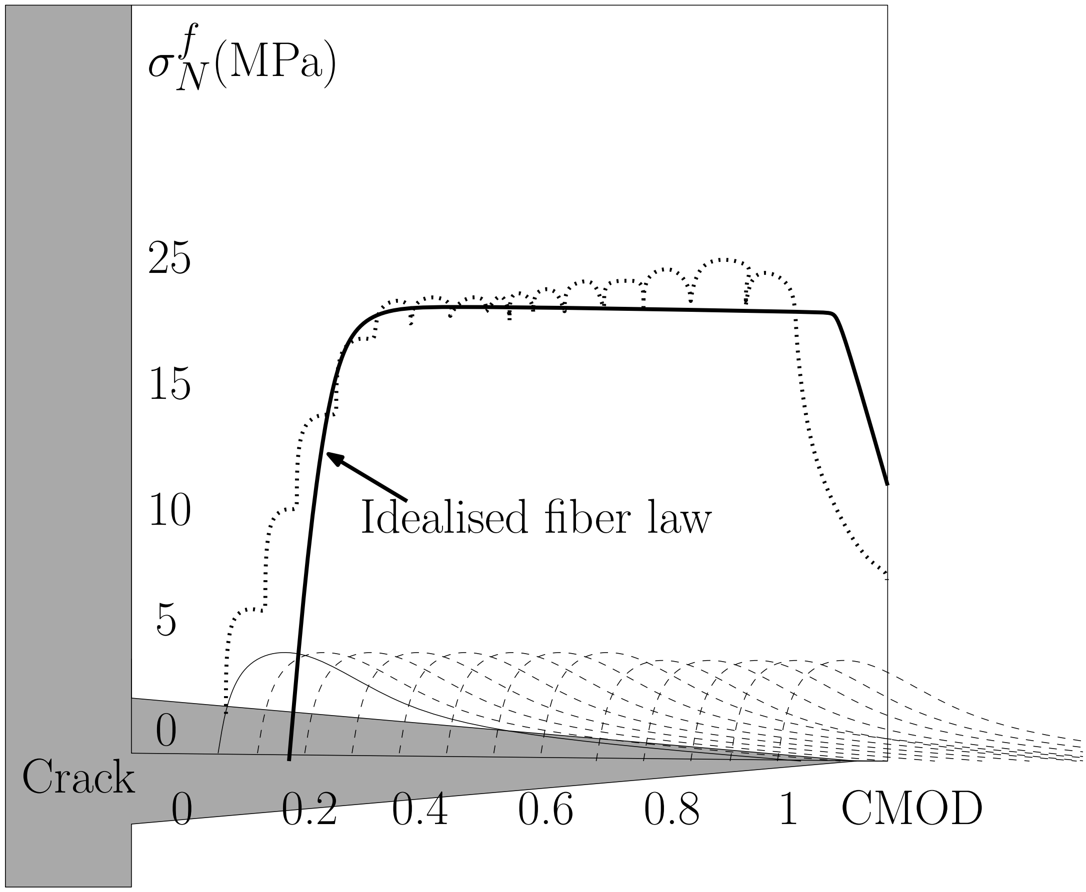

Figure 6: The fiber law used in the modeling of fiber behavior obtained by gradual activation of fibers bridging an opened crack. Stages: Hardening, crack openings and softening. (Reproduced after Caner et al. (2013))

2.1.5 Polymer matrix and steel fibers

In the article Sabuncuoglu et al. (2015) the micro-scale finite element modeling is used to estimate the stress concentration under transverse loading in a composite composed from polymer matrix and steel fibers. Three different packing types of fibers were considered: single fiber in a matrix, hexagonally packed and randomly packed fibers. The fibers had either circular or hexagonal cross-sectional shape. For the model of a single fiber, the dimensions of the model were 15 times the diameter of the fiber in the transverse directions to prevent the edge effect on the stress distribution, while the hexagonal and random fiber packing types includes $30–35$ fibers per representative volume to adequately represent the behavior of the random composite. There were large contrast between fiber and matrix stiffness: the matrix material, epoxy, had Young's modulus of 3 GPa, while it is for steel fibers 193 GPa. In the finite element meshing two layers of fiber–matrix interface regions were generated and dense mesh with equally sized elements was constructed in these regions since some of the fibers could locate close to each other. The width of these elements was 0.005 times the fiber diameter and matrix material properties were assigned to these elements. They were assumed to be perfectly bonded to the fibers and the rest of the matrix.

2.2 Category 2

The materials in category 2 contain the matrix of primary material and dispersed secondary particles (fillers) that decrease the mechanical properties of primary material. Secondary material may be containing added fillers or impurities that are not extracted from raw material. The porosity and flaws in the matrix is also considered as an example of this category. Printing paper containing clay filler and porous bone structure are examples presented in this section.

2.2.1 Paper and fillers

The filler pigments are incorporated into paper to reduce the raw material cost and improve the paper's optical properties. However, addition of the high filler amount in the paper causes loss of strength, bulk and stiffness. For unfilled paper, the semi-empirical Page equation (Page (1969)) for tensile strength of paper is widely and successfully used. Page derived his model starting from the experimental observation that tensile strength is proportional to the fraction of broken fibers across the rupture zone depending on both the strength of individual fibers and the strength of the bonds between them. The equation is function of zero-span tensile strength, area of average fiber cross section, relative bonded area, density of fibers, fiber width, perimeter of the fiber cross section and shear bond strength per unit bonded area (breaking stress of bonds). In principally, the fiber-fiber bonding is responsible for the internal cohesion of a paper sheet and technologically the inter-fiber bonding is easier alter than fiber properties (see, e.g., Retulainen & Ebeling (1993); Alava & Niskanen (2006)). The effects of filler on tensile strength were considered through a modified Page Equation by Beazley et al. (1975) and Li et al. (2002). The inter-fiber bonding strength is traditionally assumed to depend on two independent factors: bonded area and specific bond strength (see Nordman (1958)). In derivation of the modified equation for filler addition, it was assumed that reduction on strength is proportional to the total surface area of filler in the sheets. The sum of specific bond strength between available surface areas of filler and fibers and between available surface areas of free fibers and fibers are combined to replace the shear bond strength per unit bonded area. In the model, it was assumed that the filler/fiber specific shear bond is zero for inorganic fillers. Thus in the modified equation, the effect of filler on the paper tensile strength depends solely on the filler particle size and the amount of fillers in a paper sheet. In the study of Yoon (2007) the modified Page theory was found suitable to model tensile strength improvement of paper filled with clay-starch composite filler, see Figure 7.

Attempts to simulate paper properties by 3D structural model including treatments for fibers, fines and fillers have been presented by Nilsen et al. (1998), Niskanen et al. (1997), and Lavrykov et al. (2012). In KCL-PAKKA model the three-dimensional paper sheet structure is formed by deposing single fibers of rectangular cross-section randomly on a flat surface. Each fiber with defined bending stiffness is let to settle freely as low as possible without deforming the underlying sheet. The modeled artificial 3D sheet has been used for simulations of porosity and gas diffusion through sheet (Hellen et al. (2002)) and light scattering (Nilsen et al. (1998)). Hjelt et al. (2008) utilized KCL-PAKKA simulation to estimate the effect of filler clusters on bulk of a sheet. Lavrykov et al. (2012) unified several models to generate 3D fiber networks for simulations of mechanical properties. Separate approaches for formation of representative structure of hand sheet and machine sheet were presented. A set of objects was defined for the hand sheet simulations: fibers having non-collapsed or collapsed structure and fines and fillers having only one finite element in thickness direction. In machine sheet formation simulations the three-dimensional Navier-Stokes equations were used to describe the fluid motion of fiber suspension. Different boundary conditions were applied to simulate different processes in paper machine forming section. The final low consistency pulp map was used as initial input data for the network compression model implemented by LS-DYNA program (Hallquist (2006)). The elastic modulus was determined from fiber network by simulating the physical tensile test (Lavrykov et al. (2012)).

2.2.2 Porosity and multi-scale modeling

Podshivalov et al. (2011) proposed a multi-scale finite element approach for porous bone structure, which provides continuous bi-directional transition between micro- and macro-scales using intermediate scales. Firstly, the approach comprise hierarchical geometric model from a low topological complexity of macro-scale to high topological complexity of micro-scale porous structure, based on a hierarchical representation, such as octree. Secondly, the multiscale material properties model preserves effective material properties at all scales. The multiscale finite element method

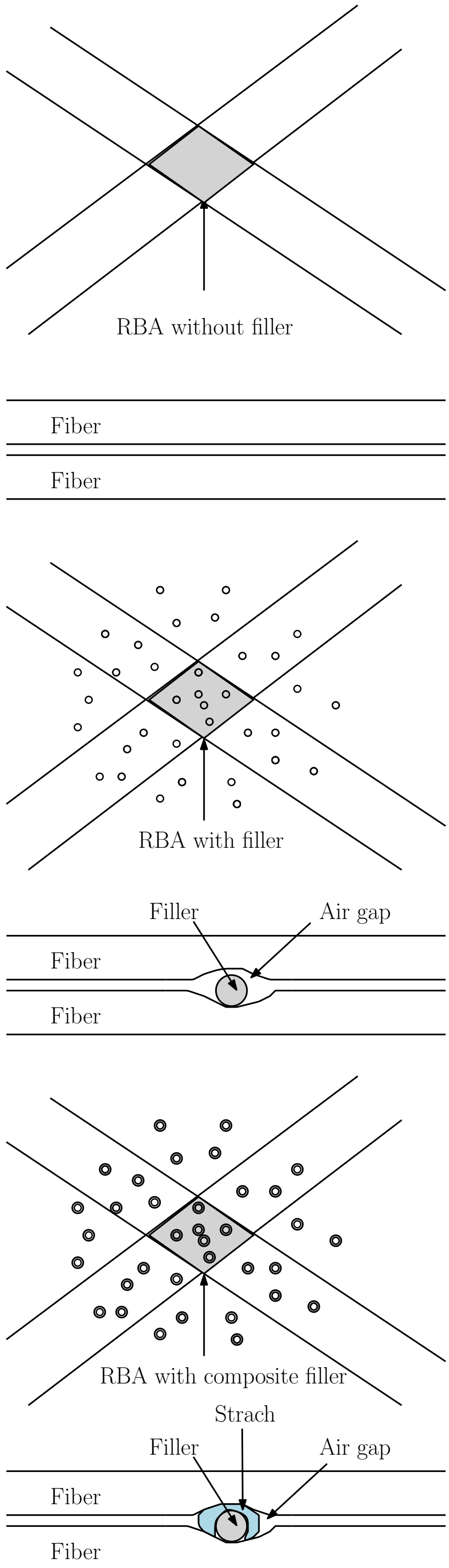

Figure 7: The relative bond area (RBA) between two fibers in the absence and presence of filler or composite filler particles. (Reproduced from Yoon (2007))

is created by integrating these two models. The geometric representation is subdivided into sub-domains using a non-overlapping domain-based method. A 3D surface mesh of sub-domains of measured micro-CT image was converted into a volumetric model by voxelization approach (Morris & Salisbury (2008)) and then into a multiresolution hierarchical volumetric model. For 3D hierarchical data structures the linear octree implementation by extending the method presented in Gargantini (1982) was used. The local material properties change to compensate the geometry modifications in intermediate scales so that effective material properties are preserved. The approach follows partially the representative volume element (RVE) homogenization method (Aboudi (2013)) and consists of four stages: RVE homogenization, effective material properties model, inverse local material properties model and computational model verification using strain-energy comparison.

Some of the analytical micromechanical models presented in Section 2.1.2 for fiber inclusion have also applied for porous structures. Eshelby's tensor and Mori-Tanaka's mean field theory have been frequently applied to estimate effective elastic properties for porous structures (see, e.g., Nemat-Nasser & Taya (1981), Nemat-Nasser et al. (1982), Zhao et al. (1989, 2005), Ichitsubo et al. (2002)). The generalized self-consistent method was used to predict the effective elastic constants of the nanoporous/cellular materials with aligned cylindrical nanopores in Duan et al. (2006).

2.3 Category 3

In the category 3 the both the matrix and reinforcing or secondary phase material has a continuous nature. The modeling of steel reinfoced concrete beam and panel have presented as an examples of this category.

2.3.1 Steel reinforced concrete

One of the recent studies for steel reinforced concrete is presented in the article Ooi & Yang (2011). In their study, the hybrid finite element–scaled boundary finite element method (FEM-SBFEM) (Song & Wolf (1999), Ooi & Yang (2010)) is utilized to model multiple cohesive crack propagation in reinforced concrete.

A discretisation is depicted in Figure 8. For the concrete bulk and reinforcement the discretisation follows standard procedure in the FEM. Fracture process zone in concrete is represented by the fictitious crack model presented in Hillerborg et al. (1976), and softening function follows bilinear curve presented in Petersson (1981). The concrete-reinforcement interaction affects both the load-carrying capacities of reinforced concrete and the prediction of crack patterns. Two stress transfer mechanisms are considered: local bond-slip and tensile splitting cracks modeled based on cohesive interface elements (CIE) (Xie (1995)). The CEB-FIP Model Code for shear stress-relative slip relation (MC90 (1993)) and empirical relationship for residual tensile strength between faces of the splitting crack (Giuriani et al. (1991)) are used. The concrete bulk mesh includes SBFEM rosettes modeling crack-tip areas. In the crack propagation criterion the crack propagation condition is satisfied if the exter-

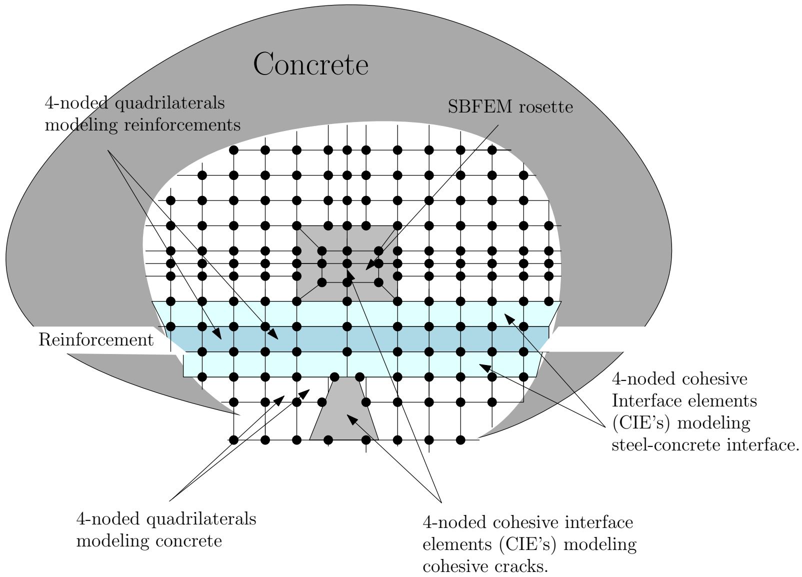

Figure 8: Discretization of cracked reinforced concrete using the hybrid FEM–SBFEM. (After Ooi & Yang (2011))

nal driving forces exceed the cohesive tractions. To avoid the evaluation of stresses at the mathematical tip of the crack, the growth of the cohesive zone is governed by requiring the stress intensity factors at the tip of the cohesive zone to vanish (Moës & Belytschko (2002)). Remeshing involves an addition of a new node to split the old crack-tip node and locating the new crack tip in the direction of crack propagation. After remeshing the crack-tip elements are replaced by SBFEM rosettes.

Tanapornraweekit et al. (2007) presented a numerical analysis of the reinforced concrete panel subjected to blast loads. N16 reinforcing bars@120 mm spacing were distributed in two directions inside both faces of the $1.19\,\mathrm{m} \times 2.19\,\mathrm{m} \times 0.14\,\mathrm{m}$ panel. The concrete model Crawford & Malvar (2006) considered three failure surfaces: initial yield failure surface, maximum failure surface and residual failure surface. A total of eight parameters in surface equations define the three failure surfaces. The stress difference at each failure surface depends on pressure in a particular element. An elastic-perfectly plastic material model was chosen to represent the steel reinforcement. The full bond interface condition between reinforcement and concrete was assumed. The boundary conditions of supports were arranged by restraining the translation in the x- and y-directions at nodes located at the positions of the center line of the tested RC panel. Bending behavior of the 140 mm panel were captured under dynamic blast loading by using commercial software LS-DYNA (Hallquist (2006)).

2.4 Category 4

The examples presented in Category 4 concern the models for flakeboards (particle board, strand/flake based composites, oriented strand board (OSB)) and wood plastic composites. Flakeboard products are widely used for applications of sheathing and construction of buildings and furniture. Particle board is made by mechanically pressing into sheet form consisting of wood fragments such as wood chips, sawmill shavings or saw dust and a synthetic resin or a suitable binder. Particle board is cheaper, denser, more uniform and lighter but also weaker than conventional wood and plywood.

Oriented strand board is engineered wood panel formed with the help of waterproof adhesives by rectangular wood strands arranged in cross-oriented layers. Its strength and structural performance is similar to plywood, but it is more uniform and less expensive. Irreversible edge swelling has been the biggest disadvantage of OSB.

Wood plastic composites (WPC) and composite lumbers are produced by mixing wood particles, heated thermoplastic resin and additives. Although WPC absorb water into to wood fibers embedded within the thermoplastic matrix material, they are dimensionally stable under moisture conditions. Other advantages are, for example, increased rot, decay and splinter resistance as well as low maintenance and the ability of the material to be molded to meet almost any desired shape. Disadvantages includes lower stiffness than wood, creed, thermal expansion and sensitivity to staining. It is still a material lacking a long-term track record of use; for example, it is possible that the strength and stiffness may be reduced by moisture absorption and freeze-thaw cycling.

2.4.1 Mechanical strength properties of particleboard

The processing parameters (surface and core moisture, pressing time, and press temperature) and structural parameters (particle size and density, mixture ratio of raw materials, and resin content) can strongly affect on mechanical strength properties of particleboard. Thus, the effect of structural and processing parameters on modulus of elasticity (MOE), bending strength (modulus of rupture, MOR) and internal bond strength (IB) of particleboard have been studied both empirical and theoretical models in number of papers. Theoretical models for predicting oriented strand board MOE data have been presented by Xu & Suchsland (1998) and Xu (1999). Empirical relationships have been developed to predict mechanical strength properties based on physical properties (see, e.g., Halligan & Schniewind (1974), Cai et al. (2004)) or based on some structural and processing parameters of particleboard (see, e.g., Barnes (2001, 2002), Lehman (1974), Hoover et al. (1992), Nirdosha & Setunge (2006)). Wong et al. (2003) used the fundamental properties of homo-profile particleboards as the basic input for the two-dimensional finite element method analysis. The modulus of elasticity of samples with different conventional density profiles was calculated using FEM. Multiple regression analysis was then conducted to estimate MOE from various density profile defining factors. In the study of Arabi et al. (2010), the MOR and MOE in particleboard were predicted from structural parameters (particle size, density, and percentage of adhesive) by a regression model based on semi-empirical Buckingham's pi-theorem. Neural networks have been applied to predict mechanical strength properties of particle board using data of measured physical properties (Fernández et al. (2008)) or process variables (Esteban et al. (2009), Cook & Chiu (1997)) as input variables.

2.4.2 Strand-based composites

Analytical micromechanical models developed for conventional composites, such as the Rule of Mixtures and the Halpin-Tsai equation (see Section 2.1.2) are applied for predicting the flexural modulus of oriented strand board (OSB) in Fan & Enjily (2009), Mundy & Bonfield (1998), Halpin & Kardos (1976), and Shaler & Blankenhorn (1990). In OSB systems, the adhesive is considered matrix and flakes are as fibers i.e. OSB is treated as a composites consisting of very high volume fractions of wood strands. Suitability of Rule of Mixtures and the Halpin-Tsai equation for OSB systems have been discussed, e.g., by Malekmohammadi et al. (2014) and Fan & Enjily (2009). Micromechanical models have combined with lamination theory by Lee & Wu (2003), Chen et al. (2008), Benabou & Duchanois (2007), Stürzenbecher et al. (2010) in order to consider an orientation distribution of the strands or a non-uniform vertical density distribution.

In Yapici et al. (2009) designed fuzzy logic classifier model to predict the effect of flake mixture ratios on the MOE and MOR. In the article Nairn & Le (2009), numerical material point method (MPM) modeling to calculate the mechanical properties of OSB as a function of strand surface geometry variations and of the blue line properties was presented. Wu et al. (2004) combined laminated model with finite element analysis to predict the effect of voids on engineering constants of OSB. Strand matrix was containing regularly spaced through-thickness cylindrical voids. In the article Wu et al. (2006), the shapes and distribution of voids is determined based on x-ray tomography analysis. Then the anisotropic mechanical properties of OSB composite are calculated using finite element analysis.

To predicted the tensile stiffness and strength of the composite boards, finite element approach was used to model the strands and resin of the composite with a substructuring routine to take advantage of the composite's repeating nature by Triche & Hunt (1993). Based on the statistics of test results, Zhu et al. (2005) used an elasto-plastic constitutive model in the finite element simulations of a load test on a compression and a nonlinear buckling analysis of OSB I-beam.

In the article Sebera et al. (2014) is applied two different geometry generation techniques for building the parametric finite element model to study an influence of material properties and strands orientations of OSB on MOE. In the first model the strand mat was generated through the volume entities. The strands were intersected and subtracted from each other using Boolean algebra and the resulting mat was meshed using free meshing. Coupled bonds were needed to connect strongly heterogeneous meshes in adjacent layers. In the second FE model the strand were created using ANSYS selection logic and the model was build via mapped finite element mesh. In the models the strands were perfectly bonded together within a layer and adhesive material was not considered. Orientation of strands rages between -20 and 20 degrees following Gauss probability distribution. The first model exhibited very high error and was rejected in the end, while the second model was found to be more suitable for strand composites modeling.

2.4.3 Composite lumber

In the article Gereke et al. (2012), the authors introduced a multiscale modeling approach, composed of two steps, for composite lumber made of wood strands. The first step estimates the effective elastic properties of a unit cell, which incorporates both the wood and resin phases using concepts of numerical homogenization with periodic boundary conditions. The second step consists of a macroscopic finite element structural analysis of a beam having random distribution of strand orientation. To improve the first step of approach, Gereke et al. (2012) and Malekmohammadi et al. (2014) presented two scenarios for partial coverage modeling: Dai's model (Dai et al. (2007)) for resin area coverage and constant resin thickness, and analytical approach based on the material morphology representation. The constant resin thickness i.e. the full resin coverage scheme is based on a combination of Voigt and Reuss models (Tucker III & Liang (1999)) and isostress and isostrain conditions between the blocks. The full coverage equations are used for partially covered strands resin using equivalent properties based on the concept of interface displacement jumps and strand and resin parameters described by Hashin (1990) and Nairn (2007), respectively. The derived analytical expressions for orthotropic elastic discontinuous rectangular shaped strand composites were also used to estimate the viscoelastic properties of a material unit cell.

2.5 Category 5

Laminated composite are generally used when there is a requirement for a high strength (stiffness) to weight ratio, because their properties can be tailored to specific structural requirements. The anisotropy of composites offers a significant enhancement in their performance over conventional materials. Laminated composite plates, which offer good in-plane properties, are prone to delamination due to their poor mechanical properties in the thickness direction. Models either predict the mechanical properties of structural laminated composite for design purposes or predict failure such as delamination, maximum transverse deflection, buckling load, failure load, natural frequency. Onset of failure in composite laminated plates requires the accurate prediction of local stress state at inter-lamina interface and in the individual lamina, which may be crucial for a safe design of the component. Review of basic derivations for determining the effective three-dimensional mechanical properties of laminated composites can be found from Bogetti et al. (1995). There is also few commercial modeling tools specially designed for analysis and design of composite laminate structures, such as NX laminate composites and LAP.

2.5.1 Plate models

The theories based on approximating the displacement distribution in thickness direction continuously differentiable varying functions are named C_z^1 function theories. The standard models of this type are the Classical Lamination Theory (CLT) and the First Order Shear Deformation Theory (FSDT). In both of these models the in-plane displacement vary linearly in thickness direction, while the transverse displacements remain constant. Although CLT and FSDT provides sufficient description of local laminate response for thin and moderately thick plates, they are not capable for direct calculation of transverse stresses with acceptable accuracy. To overcome this deficiency, a large number of so-called Higher Order Theories have been developed using consecutively higher order polynomials or other functions with continuous derivatives (see, e.g., Reddy (1984), Pandya & Kant (1988)).

If slenderness ratios are small, it have been observed that in-plane displacements show a pronounced layer-wise zigzagging implying that in-plane displacements cannot be captured by C_z^1 function theories (Pagano (1970a), Pagano & Hatfield (1972)). To overtake these difficulties the layerwise theories, which consider each layer separately, have been developed. Several models have been proposed for stress distributions and displacement over each layer thickness separately leading to functions of the in-plane coordinates. C_z^0 function theories are formulated for displacement continuity at layer interfaces (see, e.g., Reddy (1987), Ahmed & Basu (1994)).

A general consideration of hierarchical plate theory for homogenous plates can be find in Szabó & Sahrmann (1988) and an extension of hierarchical method for computing laminated composite plates was given by Babuška et al. (1992) and Actis et al. (1999). In hierarchic plate theory models the displacements are formulated into power series in thickness direction so that the interface conditions can be satisfied only approximately. The transverse functions are derived to degree in which the three-dimensional elasticity equilibrium equations are satisfied. The number of functional degrees-of-freedom increases with the degree of accuracy.

In the articles Mohite & Upadhyay (2004) and Mohite & Upadhyay (2006), authors compared a family of plate models available for the analysis of laminated structures: higher-order-shear-deformable (HSDT) model, hierarchic model and layer-wise model based on representative models adopted from Reddy (1984), Actis et al. (1999), and Ahmed & Basu (1994), respectively. Point-wise data such as transverse deflection, local state of stress and failure load produced by each model were compared to results of previous studies by Pagano & Hatfield (1972), Pagano (1970a,b), and Reddy & Reddy (1992). The layer-wise theory found to capture accurately the local state of stress for different plate thicknesses.

3 General considerations of composite modeling

Although there is plenty of empirical models based on regression analysis or some other dependencies and theoretical and analytical functions, this conclusion focus on numerical methods, especially on finite element analysis, because its applicability on vast amount of materials with different behavior (see, e.g., Shanks (2010)). In brittle and semi-brittle materials the cracking phenomena is important determining also the softening of material, but also very challenging task needing special treatment of crack tip area and the remeshing while crack propagates. In microscale matrix material, reinfocement material and bonds can be treated uniquely, but usually only small fractions can be treated that way without turning simulations very time consuming. Usual technique to treat macroscale is homogenization i.e. defining effective material properties of representative volume element, characterizing the material behavior as continuum. Laminate techniques often treat material as 2D structures decreasing that way the model complexity.

Considering real three dimensional modeling, the interesting approach was steel reinforcement concrete, where steel reinforcement, concrete and interface between them were meshed differently and having different material parameters, although in this case also the concrete was treated with homogenization and smeared crack approaches. Another interesting approach was hierarchic porous bone study, in which the material parameter in intermediate scales was determined by finite element simulation using different boundary conditions. The structure of material and distribution of different materials on studied section of material can be modeled, and different artificial ways to build, for example, oriented fiber distribution have been presented. 3D tomography techniques are improving and starting to provide real structures for base of mechanical modeling and hopefully improved computing will provide possibilities to take all particles, resins and bondings into account.

One approach onto this direction is presented by Erkkilä et al. (2015) and called here as *LE-model*. In this continuum model every element may include individual material properties, including plastic and viscous properties, and temperature and moisture content dependencies. In Erkkilä et al. (2015), the material properties differences were origin from local differences in moisture and anisotropy, but, in principle, the materials parameters differences could be origin from any other source, if the mechanical behavior of each individual constituent or interfacial zone is known separately. Unpublished study of Leppänen and Erkkilä appended fracture and cracking behavior under tensile stress to LE-model, which will bring the significant improvement concerning simulations of brittle materials.

References

Aboudi, J. (2013). *Mechanics of composite materials: A unified micromechanical approach*. Elsevier.

Actis, R. L., Szabo, B. A., & Schwab, C. (1999). Hierarchic models for laminated plates and shells. *Computer Methods in Applied Mechanics and Engineering*, 172(1), 79–107.

Addessi, D., Marfia, S., & Sacco, E. (2002). A plastic nonlocal damage model. *Computer Methods in Applied Mechanics and Engineering*, 191(13), 1291–1310.

Ahmed, N. U. & Basu, P. K. (1994). Higher-order finite element modelling of laminated composite plates. *International Journal for Numerical Methods in Engineering*, 37(1), 123–139.

Alava, M. & Niskanen, K. (2006). The physics of paper. *Reports on Progress in Physics*, 69(3), 669–723.

Arabi, M., Faezipour, M., Layeghi, M., Enayati, A., & Zahed, R. (2010). Prediction of bending strength and stiffness strength of particleboard based on structural parameters by Buckinghams p-theorem. *Journal of the Indian Academy of Wood Science*, 7(1-2), 65–70.

Babuška, I., Szabo, B. A., & Actis, R. L. (1992). Hierarchic models for laminated composites. *International Journal for Numerical Methods in Engineering*, 33(3), 503–535.

Bahn, B. Y. & Hsu, C.-T. T. (1998). Stress-strain behavior of concrete under cyclic loading. *ACI Materials Journal*, 95(2), 178–193.

Barnes, D. (2001). A model of the effect of strand length and strand thickness on the strength properties of oriented wood composites. *Forest Products Journal*, 51(2), 36–46.

Barnes, D. (2002). A model of the effect of fines content on the strength properties of oriented strand wood composites. *Forest Products Journal*, 52(5), 55–60.

Bažant, Z. P., Caner, F. C., Carol, I., Adley, M. D., & Akers, S. A. (2000). Microplane model M4 for concrete. I: Formulation with work-conjugate deviatoric stress. *Journal of Engineering Mechanics*, 126(9), 944–953.

Bažant, Z. P. & Gambarova, P. G. (1984). Crack shear in concrete: Crack band microflane model. *Journal of Structural Engineering*, 110(9), 2015–2035.

Bažant, Z. P. & Kim, S.-S. (1979). Plastic-fracturing theory for concrete. *Journal of the Engineering Mechanics Division*, 105(3), 407–428.

Bažant, Z. P. & Oh, B. H. (1983a). Crack band theory for fracture of concrete. *Matériaux et Construction*, 16(3), 155–177.

Bažant, Z. P. & Oh, B. H. (1983b). Microplane model for fracture analysis of concrete structures. In C. Ross (Ed.), *Proceedings of the symposium on the interaction of non-nuclear munitions with structures, U.S. Air Force Academy, Colorado Springs* (pp. 49–55).: McGregor & Werner.

Bažant, Z. P. & Planas, J. (1998). *Fracture and size effect in concrete and other quasibrittle materials*, volume 16 of *New Directions in Civil Engineering*. CRC Press.

Bažant, Z. P. & Prat, P. C. (1988). Microplane model for brittle-plastic material: I. Theory. *Journal of Engineering Mechanics*, 114(10), 1672–1688.

Bažant, Z. P. & Caner, F. C. (2005). Microplane model M5 with kinematic and static constraints for concrete fracture and anelasticity. I: Theory. *Journal of Engineering Mechanics*, 131(1), 31–40.

Beazley, K. M., Dennison, S. R., & Taylor, J. H. (1975). The influence of mineral fillers on paper strength: Its mechanism and practical means of modification. In *Preprints 11th ESPRA European Mtg. (Maastricht)* (pp. 217–241).

Beghini, A., Bažant, Z. P., Zhou, Y., Gouirand, O., & Caner, F. C. (2007). Microplane model M5f for multiaxial behavior and fracture of fiber-reinforced concrete. *Journal of Engineering Mechanics*, 133(1), 66–75.

Belytschko, T., Lu, Y. Y., & Gu, L. (1994). Element-free Galerkin methods. *International Journal for Numerical Methods in Engineering*, 37(2), 229–256.

Benabou, L. & Duchanois, G. (2007). Modelling of the hygroelastic behaviour of a wood-based composite for construction. *Composites Science and Technology*, 67(1), 45–53.

Benveniste, Y. (1987). A new approach to the application of Mori-Tanaka's theory in composite materials. *Mechanics of Materials*, 6(2), 147–157.

Bogetti, T. A., Hoppel, C. P., & Drysdale, W. H. (1995). *Three-dimensional effective property and strength prediction of thick laminated composite media*. Technical Report ARL-TR-911, U. S. Army Research Laboratory.

Budiansky, B. (1965). On the elastic moduli of some heterogeneous materials. *Journal of the Mechanics and Physics of Solids*, 13(4), 223–227.

Cai, Z., Wu, Q., Lee, J. N., & Hiziroglu, S. (2004). Influence of board density, mat construction, and chip type on performance of particleboard made from eastern redcedar. *Forest Products Journal*, 54(12), 226–232.

Caner, F. C., Bažant, Z. P., & Wendner, R. (2013). Microplane model M7f for fiber reinforced concrete. *Engineering Fracture Mechanics*, 105, 41–57.

Caner, F. C. & Bažant, Z. P. (2012). Microplane model M7 for plain concrete. I: Formulation. *Journal of Engineering Mechanics*, 139(12), 1714–1723.

Carol, I. & Bažant, Z. P. (1997). Damage and plasticity in microplane theory. *International Journal of Solids and Structures*, 34(29), 3807–3835.

Chen, S., Fang, L., Liu, X., & Wellwood, R. (2008). Effect of mat structure on modulus of elasticity of oriented strandboard. *Wood Science and Technology*, 42(3), 197–210.

Chen, W.-F. & Han, D.-J. (2007). *Plasticity for structural engineers*. J. Ross Publishing.

Chou, T.-W., Nomura, S., & Taya, M. (1980). A self-consistent approach to the elastic stiffness of short-fiber composites. *Journal of Composite Materials*, 14(3), 178–188.

Comi, C. (2001). A non-local model with tension and compression damage mechanisms. *European Journal of Mechanics – A/Solids*, 20(1), 1–22.

Comi, C. & Perego, U. (2001). Fracture energy based bi-dissipative damage model for concrete. *International Journal of Solids and Structures*, 38(36), 6427–6454.

Cook, D. F. & Chiu, C.-C. (1997). Predicting the internal bond strength of particleboard, utilizing a radial basis function neural network. *Engineering Applications of Artificial Intelligence*, 10(2), 171–177.

Cox, H. L. (1952). The elasticity and strength of paper and other fibrous materials. *British Journal of Applied Physics*, 3(3), 72–79.

Crawford, J. E. & Malvar, L. J. (2006). *Users and theoretical manual for K&C concrete model*. Technical Report TR-06-19.1, Karagozian & Case, Burbank, CA.

Cunha, V. M. C. F., Barros, J. A. O., & Sena-Cruz, J. M. (2011). An integrated approach for modelling the tensile behaviour of steel fibre reinforced self-compacting concrete. *Cement and Concrete Research*, 41(1), 64–76.

Cusatis, G., Bažant, Z. P., & Cedolin, L. (2003). Confinement-shear lattice model for concrete damage in tension and compression: I. Theory. *Journal of Engineering Mechanics*, 129(12), 1439–1448.

Cusatis, G., Pelessone, D., & Mencarelli, A. (2011). Lattice Discrete Particle Model (LDPM) for failure behavior of concrete. I: Theory. *Cement and Concrete Composites*, 33(9), 881–890.

Dai, C., Yu, C., Groves, K., & Lohrasebi, H. (2007). Theoretical modeling of bonding characteristics and performance of wood composites. Part II. Resin distribution. *Wood and Fiber Science*, 39(1), 56–70.

de Borst, R. (2002). Fracture in quasi-brittle materials: A review of continuum damage-based approaches. *Engineering Fracture Mechanics*, 69(2), 95–112.

Dong, Y., Wu, S., Xu, S. S., Zhang, Y., & Fang, S. (2010). Analysis of concrete fracture using a novel cohesive crack method. *Applied Mathematical Modelling*, 34(12), 4219–4231.

Dougill, J. W. (1976). On stable progressively fracturing solids. *Zeitschrift für angewandte Mathematik und Physik ZAMP*, 27(4), 423–437.

Duan, H. L., Wang, J., Karihaloo, B. L., & Huang, Z. P. (2006). Nanoporous materials can be made stiffer than non-porous counterparts by surface modification. *Acta Materialia*, 54(11), 2983–2990.

Einstein, A. (1906). Zur Theorie der Brownschen Bewegung. *Annalen der Physik*, 324(2), 371–381.

Einstein, A. (1911). Berichtigung zu meiner Arbeit: Eine neue Bestimmung der Moleküldimensionen. *Annalen der Physik*, 339(3), 591–592.

Erkkilä, A.-L., Leppänen, T., Hämäläinen, J., & Tuovinen, T. (2015). Hygro-elasto-plastic model for planar orthotropic material. *International Journal of Solids and Structures*, 62, 66–80.

Eshelby, J. D. (1957). The determination of the elastic field of an ellipsoidal inclusion, and related problems. *Proceedings of the Royal Society of London A: Mathematical, Physical and Engineering Sciences*, 241(1226), 376–396.

Esteban, L. G., Fernández, F. G., de Palacios, P., & Conde, M. (2009). Artificial neural networks in variable process control: Application in particleboard manufacture. *Forest Systems*, 18(1), 92–100.

Fan, M. & Enjily, V. (2009). Structural properties of oriented wood strand composite: Effect of strand orientation and modeling prediction. *Journal of Engineering Mechanics*, 135(11), 1323–1330.

Faria, R., Oliver, J., & Cervera, M. (1998). A strain-based plastic viscous-damage model for massive concrete structures. *International Journal of Solids and Structures*, 35(14), 1533–1558.

Fernández, F. G., Esteban, L. G., De Palacios, P., Navarro, M., & Conde, M. (2008). Prediction of standard particleboard mechanical properties utilizing an artificial neural network and subsequent comparison with a multivariate regression model. *Forest Systems*, 17(2), 178–187.

Fukuda, H. & Chou, T.-W. (1982). A probabilistic theory of the strength of short-fibre composites with variable fibre length and orientation. *Journal of Materials Science*, 17(4), 1003–1011.

Gargantini, I. (1982). An effective way to represent quadtrees. *Communications of the ACM*, 25(12), 905–910.

Genet, M., Marcin, L., & Ladevèze, P. (2014). On structural computations until fracture based on an anisotropic and unilateral damage theory. *International Journal of Damage Mechanics*, 23(4), 483–506.

Gereke, T., Malekmohammadi, S., Nadot-Martin, C., Dai, C., Ellyin, F., & Vaziri, R. (2012). Multiscale stochastic modeling of the elastic properties of strand-based wood composites. *Journal of Engineering Mechanics*, 138(7), 791–799.

Giuriani, E., Plizzari, G., & Schumm, C. (1991). Role of stirrups and residual tensile strength of cracked concrete on bond. *Journal of Structural Engineering*, 117(1), 1–18.

Gopalaratnam, V. S. & Shah, S. P. (1985). Softening response of plain concrete in direct tension. *ACI Journal Proceedings*, 82(3), 310–323.

Guth, E. (1939). On the hydrodynamical theory of the viscosity of suspensions. In *Proceedings of the Fifth International Congress for Applied Mechanics* (pp. 448–455).: John Wiley & Sons, Chapman & Hall.

Guth, E. (1945). Theory of filler reinforcement. *Journal of Applied Physics*, 16(1), 20–25.

Halligan, A. F. & Schniewind, A. P. (1974). Prediction of particleboard mechanical properties at various moisture contents. *Wood Science and Technology*, 8(1), 68–78.

Hallquist, J. O. (2006). *LS-DYNA theory manual*. Livermore Software Technology Corporation.

Halpin, J. C. & Kardos, J. (1976). The Halpin-Tsai equations: A review. *Polymer Engineering and Science*, 16(5), 344–352.

Hashin, Z. (1990). Thermoelastic properties of fiber composites with imperfect interface. *Mechanics of Materials*, 8(4), 333–348.

Hashin, Z. & Shtrikman, S. (1963). A variational approach to the theory of the elastic behaviour of multiphase materials. *Journal of the Mechanics and Physics of Solids*, 11(2), 127–140.

Hellen, E. K. O., Ketoja, J. A., Niskanen, K. J., & Alava, M. J. (2002). Diffusion through fibre networks. *Journal of Pulp and Paper Science*, 28(2), 55–62.

Hermans, J. J. (1967). Elastic properties of fiber reinforced materials when fibers are aligned. *Proceedings of the Koninklijke Nederlandse Akademie van Wetenschappen. Series B, Physical Sciences*, 70(1), 1–9.

Hill, R. (1964). Theory of mechanical properties of fibre-strengthened materials: I. Elastic behaviour. *Journal of the Mechanics and Physics of Solids*, 12(4), 199–212.

Hill, R. (1965). A self-consistent mechanics of composite materials. *Journal of the Mechanics and Physics of Solids*, 13(4), 213–222.

Hillerborg, A., Modeer, M., & Petersson, P.-E. (1976). Analysis of crack formation and crack growth in concrete by means of fracture mechanics and finite elements. *Cement and Concrete Research*, 6(6), 773–781.

Hjelt, T., Sirvio, J., & Saarela, M. (2008). Effect of filler clustering on paper properties. *Appita Journal*, 61(3), 209–211.

Hoover, W. L., Hunt, M. O., Lattanzi, R. C., Bateman, J. H., & Youngquist, J. A. (1992). Modeling mechanical properties of single-layer, aligned, mixed-hardwood strand panels. *Forest Products Journal*, 42(5), 12–18.

Houlsby, G. T. & Puzrin, A. M. (2000). A thermomechanical framework for constitutive models for rate-independent dissipative materials. *International Journal of Plasticity*, 16(9), 1017–1047.

Ichitsubo, T., Tane, M., Ogi, H., Hirao, M., Ikeda, T., & Nakajima, H. (2002). Anisotropic elastic constants of lotus-type porous copper: Measurements and micromechanics modeling. *Acta Materialia*, 50(16), 4105–4115.

Jirásek, M. & Patzák, B. (2001). Models for quasibrittle failure: Theoretical and computational aspects. In *Second European Conference on Computational Mechanics (ECCM-2001, Cracow)*.

Jirásek, M., Rolshoven, S., & Grassl, P. (2004). Size effect on fracture energy induced by non-locality. *International Journal for Numerical and Analytical Methods in Geomechanics*, 28(7-8), 653–670.

Kachanov, L. M. (1958). Time of the rupture process under creep conditions. *Isv. Akad. Nauk. SSR. Otd Tekh. Nauk*, 8, 26–31.

Kachanov, L. M. (1999). Rupture time under creep conditions. *International Journal of Fracture*, 97(1-4), 11–18.

Kachanov, M. (1980). Continuum model of medium with cracks. *Journal of the Engineering Mechanics Division*, 106(5), 1039–1051.

Kim, H. S., Hong, S. I., & Kim, S. J. (2001). On the rule of mixtures for predicting the mechanical properties of composites with homogeneously distributed soft and hard particles. *Journal of Materials Processing Technology*, 112(1), 109–113.

Krajcinovic, D. (1985). Continuous damage mechanics revisited: Basic concepts and definitions. *Journal of Applied Mechanics*, 52(4), 829–834.

Lavrykov, S., Lindström, S. B., Singh, K. M., & Ramarao, B. V. (2012). 3D network simulations of paper structure. *Nordic Pulp and Paper Research Journal*, 27(2), 256–263.

Lee, J. & Fenves, G. L. (1998). A plastic-damage concrete model for earthquake analysis of dams. *Earthquake Engineering & Structural Dynamics*, 27(9), 937–956.

Lee, J. N. & Wu, Q. (2003). Continuum modeling of engineering constants of oriented strandboard. *Wood and Fiber Science*, 35(1), 24–40.

Lehman, W. F. (1974). Properties of structural particleboards. *Forest Products Journal*, 24(1), 19–26.

Leite, J. P. B., Slowik, V., & Apel, J. (2007). Computational model of mesoscopic structure of concrete for simulation of fracture processes. *Computers & Structures*, 85(17), 1293–1303.

Leite, J. P. B., Slowik, V., & Mihashi, H. (2004). Computer simulation of fracture processes of concrete using mesolevel models of lattice structures. *Cement and Concrete Research*, 34(6), 1025–1033.

Lemaitre, J. (1984). How to use damage mechanics. *Nuclear Engineering and Design*, 80(2), 233–245.

Lemaitre, J. (1992). *A course on damage mechanics*. Springer, Berlin.

Lemaitre, J. & Chaboche, J.-L. (1990). *Mechanics of solid materials*. Cambridge University Press.

Li, L., Collis, A., & Pelton, R. (2002). A new analysis of filler effects on paper strength. *Journal of Pulp and Paper Science*, 28(8), 267–273.

Lilliu, G. & van Mier, J. G. M. (2003). 3D lattice type fracture model for concrete. *Engineering Fracture Mechanics*, 70(7), 927–941.

Liu, W. K., Park, H. S., Qian, D., Karpov, E. G., Kadowaki, H., & Wagner, G. J. (2006). Bridging scale methods for nanomechanics and materials. *Computer Methods in Applied Mechanics and Engineering*, 195(13), 1407–1421.

Luccioni, B., Oller, S., & Danesi, R. (1996). Coupled plastic-damaged model. *Computer Methods in Applied Mechanics and Engineering*, 129(1), 81–89.

Malekmohammadi, S., Tressou, B., Nadot-Martin, C., Ellyin, F., & Vaziri, R. (2014). Analytical micromechanics equations for elastic and viscoelastic properties of strand-based composites. *Journal of Composite Materials*, 48(15), 1857–1874.

MC90 (1993). *CEB-FIP Model Code 1990*. Thomas Telford.

Moës, N. & Belytschko, T. (2002). Extended finite element method for cohesive crack growth. *Engineering Fracture Mechanics*, 69(7), 813–833.

Mohite, P. M. & Upadhyay, C. S. (2004). Comparison of plate models for analysis of laminated composites. In *International Conference on Theoretical, Applied, Computational and Experimental Mechanics (IIT Kharagpur India)*.

Mohite, P. M. & Upadhyay, C. S. (2006). Accurate computation of critical local quantities in composite laminated plates under transverse loading. *Computers & Structures*, 84(10), 657–675.

Mori, T. & Tanaka, K. (1973). Average stress in matrix and average elastic energy of materials with misfitting inclusions. *Acta Metallurgica*, 21(5), 571–574.

Morris, D. & Salisbury, K. (2008). Automatic preparation, calibration, and simulation of deformable objects. *Computer Methods in Biomechanics and Biomedical Engineering*, 11(3), 263–279.

Mundy, J. S. & Bonfield, P. W. (1998). Predicting the short-term properties of chipboard using composite theory. *Wood Science and Technology*, 32(3), 237–245.

Murakami, S. (1988). Mechanical modeling of material damage. *Journal of Applied Mechanics*, 55(2), 280–286.

Nairn, J. A. (2007). Numerical implementation of imperfect interfaces. *Computational Materials Science*, 40(4), 525–536.

Nairn, J. A. & Le, E. (2009). Numerical modeling and experiments on the role of strand-to-strand interface quality on the properties of oriented strand board. In *Proceedings of 2009 International Conference on Wood Adhesives (Lake Tahoe, NV)*. CD-ROM.

Nemat-Nasser, S., Iwakuma, T., & Hejazi, M. (1982). On composites with periodic structure. *Mechanics of Materials*, 1(3), 239–267.

Nemat-Nasser, S. & Taya, M. (1981). On effective moduli of an elastic body containing periodically distributed voids. *Quarterly of Applied Mathematics*, 39, 43–59.

Ngo, D. & Scordelis, A. C. (1967). Finite element analysis of reinforced concrete beams. *ACI Journal Proceedings*, 64(3), 152–163.

Nguyen, G. D. (2005). *A thermodynamic approach to constitutive modelling of concrete using damage mechanics and plasticity theory*. PhD thesis, University of Oxford, Oxford.

Nilsen, N., Zabihian, M., & Niskanen, K. (1998). KCL-PAKKA: A tool for simulating paper properties. *Tappi Journal*, 81(5), 163–166.

Nirdosha, G. & Setunge, S. (2006). Formulation and process modeling of particleboard production using hardwood saw mill wastes using experimental design. *Composite Structures*, 75(1), 520–523.

Niskanen, K., Nilsen, N., Hellen, E., & Alava, M. (1997). KCL-PAKKA: Simulation of the 3D structure of paper. In *The Fundamentals of Papermaking Materials: Transactions of the 11th Fundamental Research Symposium (Cambridge, 1997)* (pp. 1177–1213).: Pira International.

Nordman, L. (1958). Bonding in paper sheets. In *Fundamentals of Papermaking Fibres: Transactions of the symposium, held at Cambridge, September 1957* (pp. 333–347).: British Paper and Board Makers' Association.

Ohmenhauser, F., Weihe, S., & Kroplin, B. (1999). Algorithmic implementation of a generalized cohesive crack model. *Computational Materials Science*, 16(1), 294–306.

Oliver, J. & Huespe, A. E. (2004). Continuum approach to material failure in strong discontinuity settings. *Computer Methods in Applied Mechanics and Engineering*, 193(30), 3195–3220.

Ooi, E. T. & Yang, Z. J. (2010). A hybrid finite element-scaled boundary finite element method for crack propagation modelling. *Computer Methods in Applied Mechanics and Engineering*, 199(17), 1178–1192.

Ooi, E. T. & Yang, Z. J. (2011). Modelling crack propagation in reinforced concrete using a hybrid finite element-scaled boundary finite element method. *Engineering Fracture Mechanics*, 78(2), 252–273.

Pagano, N. J. (1970a). Exact solutions for rectangular bidirectional composites and sandwich plates. *Journal of Composite Materials*, 4(1), 20–34.

Pagano, N. J. (1970b). Influence of shear coupling in cylindrical. Bending of anisotropic laminates. *Journal of Composite Materials*, 4(3), 330–343.

Pagano, N. J. & Hatfield, H. J. (1972). Elastic behavior of multilayered bidirectional composites. *AIAA Journal*, 10(7), 931–933.

Page, D. H. (1969). A theory for tensile strength of paper. *Tappi*, 52(4), 674.

Pandya, B. N. & Kant, T. (1988). Flexural analysis of laminated composites using refined higher-order C^0 plate bending elements. *Computer Methods in Applied Mechanics and Engineering*, 66(2), 173–198.

Peerlings, R. H. J. (1999). *Enhanced damage modelling for fracture and fatigue*. PhD thesis, Technische Universiteit Eindhoven.

Pelessone, D. (2005). *Discrete particle method*. Technical report, Engineering and Software System Solutions, Inc.

Pereira, E. N. B. (2006). Steel fibre reinforced self-compacting concrete: From material to mechanical behaviour. ResearchGate.

Petersson, P.-E. (1981). *Crack growth and development of fracture zones in plain concrete and similar materials*. PhD thesis, Lund University.

Podshivalov, L., Fischer, A., & Bar-Yoseph, P. Z. (2011). 3D hierarchical geometric modeling and multiscale FE analysis as a base for individualized medical diagnosis of bone structure. *Bone*, 48(4), 693–703.

Ramadoss, P. & Nagamani, K. (2012). Modeling for the evaluation of strength and toughness of high-performance fiber reinforced concrete. *Journal of Engineering Science and Technology*, 7(3), 280–291.

Rashid, Y. R. (1968). Ultimate strength analysis of prestressed concrete pressure vessels. *Nuclear Engineering and Design*, 7(4), 334–344.

Reddy, J. N. (1984). A simple higher-order theory for laminated composite plates. *Journal of Applied Mechanics*, 51(4), 745–752.

Reddy, J. N. (1987). A generalization of two-dimensional theories of laminated composite plates. *Communications in Applied Numerical Methods*, 3(3), 173–180.

Reddy, Y. S. N. & Reddy, J. N. (1992). Linear and non-linear failure analysis of composite laminates with transverse shear. *Composites Science and Technology*, 44(3), 227–255.

Reinhardt, H. W., Cornelissen, H. A. W., & Hordijk, D. A. (1986). Tensile tests and failure analysis of concrete. *Journal of Structural Engineering*, 112(11), 2462–2477.

Retulainen, E. & Ebeling, K. (1993). Fibre-fibre bonding and ways of characterizing bond strength. *Appita*, 46(4), 282–288.

Reuss, A. (1929). Berechnung der Fließgrenze von Mischkristallen auf Grund der Plastizitätsbedingung für Einkristalle. *ZAMM – Journal of Applied Mathematics and Mechanics / Zeitschrift für Angewandte Mathematik und Mechanik*, 9(1), 49–58.

Sabuncuoglu, B., Orlova, S., Gorbatikh, L., Lomov, S. V., & Verpoest, I. (2015). Microscale finite element analysis of stress concentrations in steel fiber composites under transverse loading. *Journal of Composite Materials*, 49(9), 1057–1069.

Salari, M. R., Saeb, S., Willam, K. J., Patchet, S. J., & Carrasco, R. C. (2004). A coupled elastoplastic damage model for geomaterials. *Computer Methods in Applied Mechanics and Engineering*, 193(27), 2625–2643.

Schlangen, E. & Van Mier, J. G. M. (1992a). Experimental and numerical analysis of micromechanisms of fracture of cement-based composites. *Cement and Concrete Composites*, 14(2), 105–118.

Schlangen, E. & Van Mier, J. G. M. (1992b). Simple lattice model for numerical simulation of fracture of concrete materials and structures. *Materials and Structures*, 25(9), 534–542.

Sebera, V., Tippner, J., Kunecký, J., Muzsyński, L., & Rademacher, P. (2014). FE model of oriented strand board made by two different geometry generation techniques. In H. M. Barnes & V. L. Herian (Eds.), *Proceedings of the 57th International Convention of Society of Wood Science and Technology (Zvolen, 2014)* (pp. 821–827).

Shaler, S. M. & Blankenhorn, P. R. (1990). Composite model prediction of elastic moduli for flakeboard. *Wood and Fiber Science*, 22(3), 246–261.

Shanks, R. A. (2010). Modelling of polymeric fibre-composites and finite element simulation of mechanical properties. In D. Moratal (Ed.), *Finite Element Analysis* (pp. 285–314). Sciyo Publishing, Rijeka.

Simo, J. C. & Ju, J. W. (1987). Strain-and stress-based continuum damage models – I. Formulation. *International Journal of Solids and Structures*, 23(7), 821–840.

Song, C. & Wolf, J. P. (1999). The scaled boundary finite element method – alias consistent infinitesimal finite element cell method for diffusion. *International Journal for Numerical Methods in Engineering*, 45(10), 1403–1431.

Stürzenbecher, R., Hofstetter, K., Schickhofer, G., & Eberhardsteiner, J. (2010). Development of high-performance strand boards: Multiscale modeling of anisotropic elasticity. *Wood Science and Technology*, 44(2), 205–223.

Sukumar, N., Moës, N., Moran, B., & Belytschko, T. (2000). Extended finite element method for three-dimensional crack modelling. *International Journal for Numerical Methods in Engineering*, 48(11), 1549–1570.

Szabó, B. A. & Sahrmann, G. J. (1988). Hierarchic plate and shell models based on p-extension. *International Journal for Numerical Methods in Engineering*, 26(8), 1855–1881.

Tanapornraweekit, G., Haritos, N., Mendis, P., & Ngo, T. (2007). Modelling of a reinforced concrete panel subjected to blast load by explicit non-linear FE code. In *Proceedings of AEES 2007 Conference*: Australian Earthquake Engineering Society.

Tandon, G. P. & Weng, G. J. (1984). The effect of aspect ratio of inclusions on the elastic properties of unidirectionally aligned composites. *Polymer Composites*, 5(4), 327–333.

Taylor, G. I. (1938). Plastic strain in metals. *Journal of the Institute of Metals*, 62, 307–324.

Triche, M. H. & Hunt, M. O. (1993). Modeling of parallel-aligned wood strand composites. *Forest Products Journal*, 43(11, 12), 33–44.

Tucker III, C. L. & Liang, E. (1999). Stiffness predictions for unidirectional short-fiber composites: Review and evaluation. *Composites Science and Technology*, 59(5), 655–671.

Voigt, W. (1889). Ueber die Beziehung zwischen den beiden Elasticitätsconstanten isotroper Körper. *Annalen der Physik*, 274(12), 573–587.

Weihe, S., Kroplin, B., & De Borst, R. (1998). Classification of smeared crack models based on material and structural properties. *International Journal of Solids and Structures*, 35(12), 1289–1308.

Wong, E.-D., Yang, P., Zhang, M., Wang, Q., Nakao, T., Li, K.-F., & Kawai, S. (2003). Analysis of the effects of density profile on the bending properties of particleboard using finite element method (FEM). *Holz als Roh- und Werkstoff*, 61(1), 66–72.

Wu, Q., Lee, J. N., & Han, G. (2004). The influence of voids on the engineering constants of oriented strandboard: A finite element model. *Wood and Fiber Science*, 36(1), 71–83.

Wu, Q., Zhang, B., Wang, L., & Han, G. (2006). The application of 3-D X-ray tomography with finite element analysis for engineering properties of strand-based composites. In *Advances and Challenges in Biocomposites: Proceedings of the 8th Pacific Rim Bio-based Composites Symposium* (pp. 200–209).

Xie, M. (1995). *Finite element modeling of discrete crack propagation*. PhD thesis, University of New Mexico.

Xu, W. (1999). Influence of vertical density distribution on bending modulus of elasticity of wood composite panels: A theoretical consideration. *Wood and Fiber Science*, 31(3), 277–282.

Xu, W. & Suchsland, O. (1998). Modulus of elasticity of wood composite panels with a uniform vertical density profile: A model. *Wood and Fiber Science*, 30(3), 293–300.

Yapici, F., Ozcifci, A., Akbulut, T., & Bayir, R. (2009). Determination of modulus of rupture and modulus of elasticity on flakeboard with fuzzy logic classifier. *Materials & Design*, 30(6), 2269–2273.

Yoon, S.-Y. (2007). *Bonding material coated clay for improving paper properties*. PhD thesis, Georgia Institute of Technology.

Zaoui, A. (2002). Continuum micromechanics: Survey. *Journal of Engineering Mechanics*, 128(8), 808–816.

Zhao, Y., Taya, M., Kang, Y., & Kawasaki, A. (2005). Compression behavior of porous NiTi shape memory alloy. *Acta Materialia*, 53(2), 337–343.

Zhao, Y. H., Tandon, G. P., & Weng, G. J. (1989). Elastic moduli for a class of porous materials. *Acta Mechanica*, 76(1-2), 105–131.

Zhu, E., Guan, Z., Rodd, P., & Pope, D. (2005). A constitutive model for OSB and its application in finite element analysis. *Holz als Roh- und Werkstoff*, 63(2), 87–93.